

## Magnetic properties of ultrathin Ni films

O. V. Snigirev, A. M. Tishin, and K. E. Andreev

*M. V. Lomonosov Moscow State University, 119899 Moscow, Russia*

S. A. Gudoshnikov

*Institute of Earth Magnetism, the Ionosphere, and Radio Wave Propagation, Russian Academy of Sciences, 142092 Troitsk, Moscow Region, Russia*

J. Bohr

*Technical University of Denmark, DK 2800 Lyngby, Denmark*

(Submitted November 20, 1997; resubmitted March 11, 1998)

*Fiz. Tverd. Tela (St. Petersburg)* **40**, 1681–1685 (September 1998)

The magnetic properties of Au/Ni/Si(100) films with Ni thicknesses of 8–200 Å are studied at  $T = 77$  K using a scanning magnetic microscope with a thin-film high-temperature dc SQUID. It is found that the Ni films, with an area of  $0.6 \times 0.6$  mm, which are thicker than 26 Å have a single-domain structure with the magnetic moment oriented in the plane of the film and a saturation magnetization close to 0.17 MA/m. For films less than 26 Å thick, the magnetization of the film is found to drop sharply. © 1998 American Institute of Physics. [S1063-7834(98)02509-X]

Studies of the properties of ultrathin magnetic films are of fundamental, as well as practical, interest. These films can be used in magnetic recording devices to enhance the memory density. From the standpoint of fundamental research, these films are interesting objects for studying magnetic ordering in two-dimensional (2D) magnets.<sup>1,2</sup>

The best known devices for measuring the magnetic properties of ultrathin films, the surfaces of 3d and 4f metals, and submicron particles of recording media can be classified into three groups: devices used to measure the integrated magnetic moment of a sample;<sup>3–5</sup> devices which produce an image of the structure of magnetic objects with high spatial resolution;<sup>6–9</sup> and, instruments using synchrotron or neutron radiation.<sup>10–12</sup>

Recently developed scanning SQUID-microscopes<sup>13</sup> make it possible to measure the absolute magnitude of the magnetization of a sample with a high sensitivity that is not accessible to other devices and to take topograms of the magnetic field of a test object with a spatial resolution down to a few micrometers.<sup>14</sup>

In this paper we present the results of a study of the magnetic properties of ultrathin Au/Ni/Si(100) films at a temperature of 77 K using a SQUID-microscope.

### 1. PROPERTIES OF THIN Ni FILMS

Thin Ni films can have two types of crystal structure [face centered (*fcc*) and body centered (*bcc*)] with substantially different magnetic properties.<sup>15</sup> According to theory, *fcc* Ni exists only in a ferromagnetic phase, while the *bcc* modification displays a transition from a ferromagnetic to a nonmagnetic phase<sup>15</sup> as the Wigner–Zitz radius is lowered to a critical value on the order of 2.6 Å. A transition from the

nonmagnetic to the ferromagnetic state has also been predicted for epitaxial *bcc*-Ni films subjected to a 1% stretching of the lattice caused by the substrate.<sup>16</sup>

The magnitude and spatial orientation of the magnetic moment of Ni films depend on the number of monolayers, the substrate, and the structure of the buffer layer.<sup>8,16–19</sup>

The dimensions of the magnetic domains formed in Ni films range from tens of micrometers to a few micrometers as the thickness of the Ni is changed from 20 to 140 Å.<sup>6</sup>

Besides the above properties, ultrathin Ni films can also manifest a spectrum of phenomena associated with the transition from two-dimensional to three-dimensional magnetic systems as the number of monolayers is increased. It has been found, for example, that the value of the critical index  $\beta$  in the temperature dependence of the magnetization in the neighborhood of the phase transition,  $M(T) \propto (1 - T/T_c)^\beta$ , changes quite sharply from 0.125, which is characteristic of two-dimensional ‘‘Ising’’ magnets, to 0.43, which is characteristic of three-dimensional ‘‘Heisenberg’’ magnets, as the thickness of Ni films is varied from 5 to 10 monatomic layers.<sup>7</sup>

The Curie temperature  $T_c$  also depends on the Ni film thickness and can vary from 50 to 450 K as the thickness of Ni/Cu(001) films is increased from 1.5 to 8 monolayers.<sup>20</sup> Here the dependence of  $T_c$  on the film thickness can be extrapolated to  $T_c = 0$  for a single monolayer of Ni.<sup>21</sup>

### 2. EXPERIMENTAL TECHNIQUE

Figure 1 shows the mutual positions of the SQUID-probe<sup>22</sup> of the scanning magnetic microscope, the test sample of Ni film on a 0.3-mm-thick substrate of Si(100), and a thin-film calibration loop deposited on the same silicon substrate. The film samples were made<sup>22</sup> in the

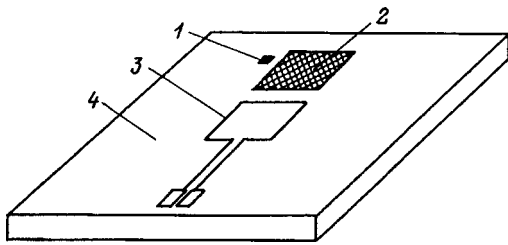


FIG. 1. Schematic illustration of the mutual positions of the SQUID (1), sample (2), and calibration loop (3) on the substrate (4) in a magnetic SQUID-microscope.

form of a square with  $600 \mu\text{m}$  edges. In order to visualize the distribution of the magnetic field created by the sample, the sample was scanned with a sample-probe distance on the order of  $100 \mu\text{m}$ .

A magnetizing field parallel to the sample plane was provided by a long solenoid, and a field perpendicular to the sample was created by a quasi-plane 500-turn coil. The scanning SQUID-microscope could normally operate in magnetic fields of up to  $70 \text{ A/m}$  for fields directed perpendicular to the plane of the SQUID (and the plane of the sample) and in fields up to  $10^4 \text{ A/m}$  oriented parallel to the SQUID.

Information on the crystallographic structure of the samples was obtained on thick Ni films ( $200 \text{ \AA}$ ) without a gold coating on a Rigaku x-ray diffractometer. Only the (111) reflection was observed ( $2\vartheta = 44.32^\circ$ ); the full width at half maximum of the peak was  $1.028^\circ$ . The existence of a single reflection (111) is evidence of a textured structure for the deposited Ni film and a strongly expressed (111)-orientation. The lattice constant calculated from the position of the  $2\theta$  reflection was  $3.53 \text{ \AA}$ . The observed (111) film orientation is natural, since in this case the mismatch between the lattice constant in the Si (100) plane ( $5.2 \text{ \AA}$ ) and the Ni atoms in the plane of its film ( $4.99 \text{ \AA}$ ) is minimal. It was not possible to check the thinner films in this manner because of the low intensity of the reflected radiation.

During the measurements, the probe of the scanning SQUID-microscope was mounted in a Dewar flask with liquid nitrogen located inside a double permalloy shield. The residual magnetic field can be measured by turning the probe around a vertical axis by  $360^\circ$ . Its maximum was close to  $2.5 \mu\text{T}$ . An alternating current of about  $300 \mu\text{A}$  was applied to the calibration coil (Fig. 1); its magnetic image could be used for mounting the sample inside the scanning field of the scanning SQUID-microscope (on the order of  $8 \times 8 \text{ mm}^2$ ). The measured magnetic field over the central portion of the coil makes it possible to determine the distance  $h$  between the sample and the SQUID, which in our experiments was varied from  $100$  to  $400 \mu\text{m}$  and determined the spatial resolution of the apparatus.

### 3. RESULTS OF THE MEASUREMENTS

The properties of Ni films with thicknesses of  $8$ – $200 \text{ \AA}$  coated with a layer of Au were studied. Images were recorded after the sample had been cooled in the residual magnetic field from a temperature  $T \approx 400 \text{ K}$  to the boiling temperature of liquid nitrogen. Scanning the  $26\text{-\AA}$ -thick film

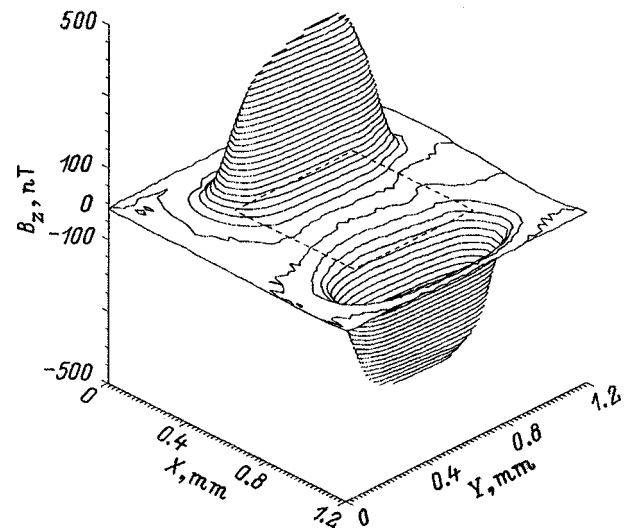


FIG. 2. Magnetic image of a  $26\text{-\AA}$ -thick,  $0.6 \times 0.6 \text{ mm}$  Ni film in an applied magnetic field of  $4000 \text{ A/m}$  directed parallel to the  $Y$  axis.

yielded a weak magnetic signal corresponding to an orientation of the magnetization vector in the plane of the film. When a magnetic field of  $4000 \text{ A/m}$  was applied parallel to the plane of the film, the signal-to-noise ratio increased to over 100 and the magnetic image became distinct (Fig. 2). Sharp peaks at the maximum and minimum of the  $B_z$  component of the magnetic field lay on opposite edges of the test film which is indicated by a dotted line in Fig. 2. The symmetry of the image (the positive and negative responses are equal in size) is a result of orienting the magnetization vector in the plane of the film. The presence of only two peaks in the magnetic image of the entire film, whose dimensions greatly exceed the spatial resolution of the scanning SQUID-microscope, can be interpreted as evidence of a single-domain structure.

The change in the component  $B_z(x,y)$ , relative to the phonon signal  $B_z(0,0)$  recorded far from the film, was calculated from the change in the output voltage  $\Delta V_{\text{out}}$  of the SQUID, the known feedback coefficient  $\Delta V_{\text{out}}/\Phi_0$  of the SQUID electronics (here  $\Phi_0$  is the quantum of magnetic flux), and the previously measured effective area  $A_{\text{eff}}$  of the SQUID.<sup>22,23</sup>

The dependence of the volume magnetization of the  $26 \text{ \AA}$  Ni film on a parallel applied field is shown in Fig. 3. This hysteresis curve was obtained by successive measurements of the peak value of  $B_z$  as the magnitude of the applied field was varied from  $+4000$  to  $-4000 \text{ A/m}$  and back. These data show that the saturation magnetization of this film is  $0.17 \text{ MA/m}$ , which is attained at a field strength of about  $2500 \text{ A/m}$ . This value of the saturation magnetization is approximately a factor of 3 smaller than that of bulk Ni. The hysteresis loop (Fig. 3) is evidence of magnetic ordering in the sample with a phase transition temperature above  $77 \text{ K}$ . The overall shape of the  $M(H)$  curve suggests that this ordering is ferromagnetic in character. The coercitive force is close to  $35 \text{ A/m}$  and the residual magnetic moment is  $0.028 \text{ MA/m}$ . When a perpendicular magnetic field with a maximum strength of  $70 \text{ A/m}$  was applied to the  $26\text{-\AA}$ -thick Ni film, the

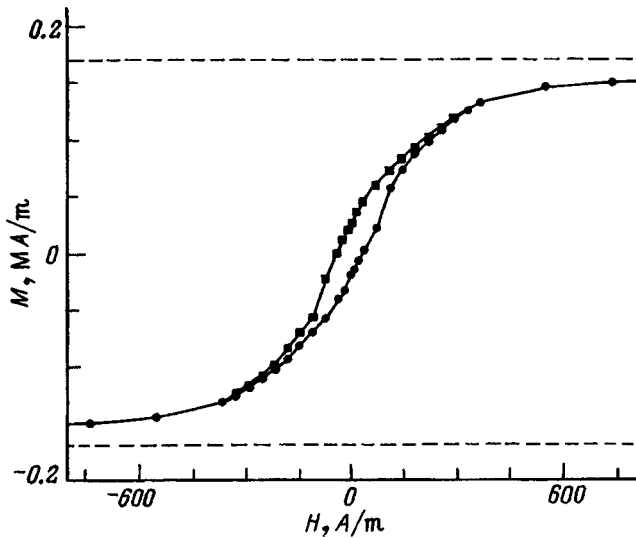


FIG. 3. Hysteresis loop of a 26-Å-thick Ni film in a parallel applied magnetic field.

signal was below the noise level of the SQUID and an image could not be obtained.

Attempts to record images of samples with thicknesses of 15 and 8 Å in parallel and perpendicular magnetic fields with distances of 100 μm between the SQUID and sample showed that their magnetizations are below the sensitivity threshold of the instrument. Thus, when the thickness of the Ni films was varied from 26 to 15 Å, the magnetization fell by more than two orders of magnitude (Fig. 4).

As opposed to the 26-Å-thick films, the images of Ni films with thicknesses of 43 and 84 Å, recorded after they were cooled in zero field, showed distinct pairs of symmetric positive and negative peaks located on opposite corners of the square film samples. These images correspond to a single-domain magnetic structure with an easy axis of magnetization lying in the plane of the film along a diagonal. When a parallel magnetizing field on the order of 4000 A/m in magnitude was applied, the magnetic moment of the film

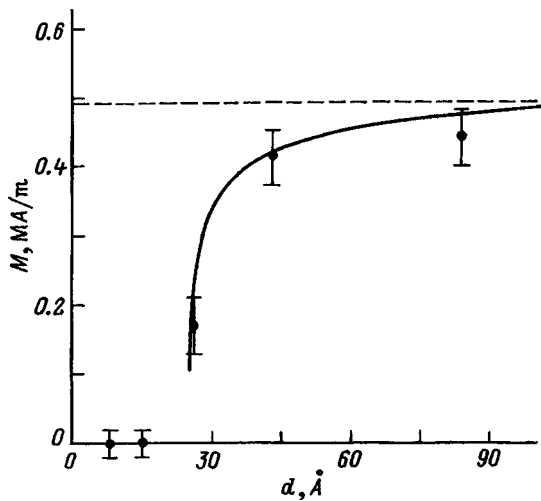


FIG. 4. Saturation magnetization as a function of Au/Ni/Si(100) film thickness.

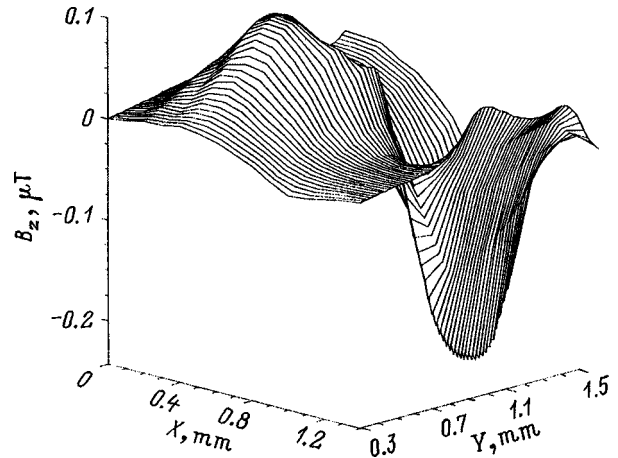


FIG. 5. Magnetic image of a 30-Å-thick Ni film deposited on a Pt buffer layer in a 4000 A/m magnetic field directed parallel to the Y axis.

rotated relative to the direction of the field and the peaks were shifted to the location indicated in Fig. 2a. Similar results were obtained for 200-Å-thick Ni films without a gold coating.

In order to determine the way the silicon substrate influences the orientation and magnitude of the magnetic moment of the film, we have prepared and studied samples of Au/Ni/Pt/Si(100) films with a 100-nm-thick buffer layer of Pt. The lattice parameter of the platinum, 3.9 Å, is in between those of Si and Ni, which reduces the stretching of the Ni layers in the film. An image of the distribution of the  $B_z$  component of the magnetic field is shown in Fig. 5.

4. DISCUSSION OF RESULTS

We begin the discussion with the simplest case of relatively thick Au/Ni/Si(100) films with thicknesses of 43 and 84 Å. As the measurements at  $T=77$  K show, ferromagnetic ordering is observed in them. Here the saturation magnetization is close to the bulk value (Fig. 4), in agreement with theory.<sup>15</sup>

The observed orientation of the magnetization in the plane of the film may be the consequence of a number of factors. First, with this orientation there is almost no demagnetization field in the film; second, because of the stretching of the Ni film by the silicon substrate, the direction of easy magnetization can lie in the plane of the film; and/or, third, 77 K lies between the magnetic phase transition point and the reorientation temperature  $T_R$  for these films.<sup>24</sup>

The domain structure of the thick films turned out to be insensitive to the applied magnetic field, regardless of whether it was directed parallel or perpendicular to the plane of the film. (In our experiments these fields were up to 4000 and 70 A/m, respectively).

Films with intermediate thicknesses (about 25 Å) also manifested ferromagnetic ordering, but with a smaller saturation magnetization. This is most likely because the sample temperature  $T=77$  K was close to the phase transition temperature for this film thickness.

An alternative reason may be an island (cluster) structure of the film, which becomes more probable as the thickness is

reduced. Ferromagnetic ordering with a magnetization oriented in the plane of the film has been observed previously with cluster radii below 30 Å, for example in rather thin (about 30 monolayers) Fe films.<sup>24</sup> Thus, the reduction in the magnetization of Ni films with thicknesses of 15–30 Å may be a result of cluster formation.

A magnetic moment corresponding to ferromagnetic ordering was not observed in the Ni films with thicknesses of 8 and 15 Å at the existing sensitivity of the scanning SQUID-microscope. It may be assumed that the magnetic phase transition point for these films lies below 77 K, although other mechanisms may play a role.<sup>5,25</sup> Perhaps, at these thicknesses the film has an island structure and is in a superparamagnetic state, as has been observed, for example, for Fe films thinner than 39 Å.<sup>5</sup> It has been conjectured<sup>5</sup> that supermagnetism is typical of magnetic films that form islands during the growth process.

The nature of the magnetic-field distribution over the surface of Au/Ni/Pt/Si films, especially the asymmetry between the positive and negative maxima, indicates the existence of a component of the magnetic moment perpendicular to the plane of the film. Thus, the presence of a buffer layer greatly changed the magnetic anisotropy energy of the film. This suggests that eliminating the stretching of the Ni monolayers leads to an orientation of the magnetic moment of a given film sample perpendicular to its plane. Besides a change in the orientation of the magnetic moment, our experimental data imply an extremely large reduction in the magnetic moment of the Ni atoms, which may indicate a substantial readjustment of the energy spectrum of films with a buffer layer.

As for the characteristics of the magnetic microscope, our results show that the sensitivity of the apparatus was sufficient to measure the hysteresis curves of films thicker than 26 Å in applied magnetic fields of magnitude  $\pm 4000$  A/m, if the field is oriented parallel to the plane of the sample and the plane of the SQUID. In the case of a perpendicular magnetizing field, it was possible to make measurements for magnetization fields no higher than 70 A/m, since in high fields the critical current of the Josephson junctions of the SQUID was suppressed. For measurements in fields higher than 100 A/m, SQUIDs with a submicron Josephson junctions must be used.

The spatial resolution in the magnetic image of the observed samples and the magnetic field resolution of the magnetic microscope used here were close to 100  $\mu\text{m}$  and  $10^{-15}$  Am<sup>2</sup>/Hz<sup>1/2</sup>, respectively. Both of these parameters can be improved by reducing the distance between the SQUID and the sample.<sup>14</sup>

In conclusion, we note that the magnetic scanning SQUID-microscopy method developed here can be used to obtain an image of the spatial distribution of one of the com-

ponents of the magnetic field of ultrathin films of magnetic materials and to determine, to a high accuracy not available with other devices, their local magnetizations in regions where the acting fields are low.

We thank S. I. Krasnosvobodtsev, L. V. Matveets, A. V. Pavolotskiĭ, I. G. Prokhorova, S. N. Polyakov, N. N. Ukhanskiĭ, and I. I. Vengrus for help in various stages of this work.

This work was supported by the Russian Fund for Fundamental Research (Projects No. 96-02-19250 and 96-02-18127a) and INTAS (Grant No. 93-2777-ext).

<sup>1</sup>N. D. Mermin and H. Wagner, Phys. Rev. Lett. **17**, 1133 (1966).

<sup>2</sup>L. Onsager, Phys. Rev. **65**, 117 (1944).

<sup>3</sup>M. Sakurai, N. Imamura, K. Hirano, and T. Shinjo, J. Magn. Magn. Mater. **147**, 16 (1995).

<sup>4</sup>R. Bergholz and U. Gragmann, J. Magn. Magn. Mater. **45**, 389 (1984).

<sup>5</sup>M. Weber, R. Koch, and K. H. Rieder, Phys. Rev. Lett. **73**, 1166 (1994).

<sup>6</sup>G. Bochi, H. J. Hug, D. I. Paul, B. Stiefel, A. Moser, I. Parashikov, H.-J. Güntherodt, and R. C. O'Handley, Phys. Rev. Lett. **75**, 1839 (1995).

<sup>7</sup>F. Huang, M. T. Kief, G. J. Mankey, and R. F. Willis, Phys. Rev. B **49**, 3962 (1994).

<sup>8</sup>G. Bochi, C. A. Ballantine, H. E. Inglefield, C. V. Thompson, R. C. O'Handley, H. J. Hug, B. Stiefel, G. Moser, and H.-J. Güntherodt, Phys. Rev. B **52**, 7311 (1995).

<sup>9</sup>A. Oral, S. J. Bending, and M. Henini, J. Vac. Sci. Technol. B **14**, 1202 (1996).

<sup>10</sup>C. F. Majkrzak, J. Kwo, M. Hong, Y. Yafet, D. Gibbs, C. L. Chien, and J. Bohr, Adv. Phys. **40**, 99 (1991).

<sup>11</sup>G. H. Lander, Invited paper submitted to the 21st Rare Earth Research Conf., Duluth, MN (July 7-12, 1996), to be published in Journal of Alloys and Compounds.

<sup>12</sup>G. M. Watson, D. Gibbs, G. H. Lander, B. D. Gaulin, L. E. Bermann, H. Matzke, and W. Ellis, Phys. Rev. Lett. **77**, 751 (1996).

<sup>13</sup>L. N. Vu, M. S. Wistron, and D. J. van Harlingen, Appl. Phys. Lett. **63**, 1693 (1993).

<sup>14</sup>J. R. Kirtley, M. B. Ketchen, K. G. Stwaisz, J. Z. Sun, W. J. Gallagher, S. H. Blanton, and S. J. Wind, Appl. Phys. Lett. **66**, 1138 (1995).

<sup>15</sup>V. L. Moruzzi, P. M. Marcus, K. Schwarz, and P. Mohn, Phys. Rev. B **34**, 1784 (1986).

<sup>16</sup>J. I. Lee, Soon C. Hong, A. J. Freeman, and C. L. Fu, Phys. Rev. B **47**, 810 (1993).

<sup>17</sup>J. Vogel, G. Panaccione, and M. Sacchi, Phys. Rev. B **50**, 7157 (1994).

<sup>18</sup>B. Schulz and K. Baberschke, Phys. Rev. B **50**, 13467 (1994).

<sup>19</sup>J. Shen, J. Giergiel, and J. Kirschner, Phys. Rev. B **52**, 8454 (1995).

<sup>20</sup>A. Aspelmeier, M. Tischer, M. Farle, M. Russo, K. Baberschke, and D. Arvanitis, J. Magn. Magn. Mater. **146**, 256 (1995).

<sup>21</sup>F. Huang, G. J. Mankey, M. T. Kief, and R. F. Willis, J. Appl. Phys. **73**, 6760 (1993).

<sup>22</sup>O. V. Snigirev, K. E. Andreev, A. M. Tishin, S. A. Gudoshnikov, and J. Bohr, Phys. Rev. B **55**, 1429 (1997).

<sup>23</sup>S. A. Gudoshnikov, N. N. Ukhanskiy, I. I. Vergrus, K. E. Andreev, A. M. Tishin, and O. V. Snigirev, IEEE Trans. Appl. Supercond. **7**, 2542 (1997).

<sup>24</sup>Ar. Abanov, V. Kalatsky, V. L. Pokrovsky, and W. M. Saslov, Phys. Rev. B **51**, 1023 (1995).

<sup>25</sup>C. P. Flynn and M. B. Salomon, Synthesis and properties of single crystal nanostructures: *Handbook on the Physics and Chemistry of Rare Earths*, Vol. 22, edited by K. A. Gschneider and L. Eyring (North-Holland, Amsterdam, 1996), Ch. 147.